European Journal of Radiology 117 (2019) 140–148

Contents lists available at ScienceDirect

European Journal of Radiology

journal homepage: www.elsevier.com/locate/ejrad

Review

Preoperative multimodality imaging of pectus excavatum: State of the art review and call for standardization

Gastón A. Rodríguez-Granillo[a,*], Marcelo Martínez-Ferro[b], Carlos Capuñay[a], Gaston Bellia-Munzón[b], Alejandro Deviggiano[a], Ignacio Raggio[c], Eduardo Fernandez-Rostello[d], Elias Hurtado Hoyo[e], Gorka Bastarrika[f], Patricia Carrascosa[a]

[a] Departament of Cardiovascular Imaging, Diagnóstico Maipú, Buenos Aires, Argentina
[b] Department of Surgery, Fundacion Hospitalaria, Private Children's Hospital, Buenos Aires, Argentina
[c] Department of Cardiology, Clínica Olivos, Buenos Aires, Argentina
[d] Hospital Rivadavia, Buenos Aires, Argentina
[e] Asociación Medica Argentina, Buenos Aires, Argentina
[f] Department of Radiology, Clínica Universidad de Navarra, Pamplona, Navarra, Spain

ARTICLE INFO

Keywords:
Chest malformation
Thoracic imaging
Diastolic function
Cardiopulmonary
Cardiac magnetic resonance
Stress-Echocardiography

ABSTRACT

Purpose: Image acquisition protocols and reports in patients with pectus excavatum (PEX) differ significantly from routine examinations, and no imaging modality can enable a comprehensive assessment of PEX severity and cardiac impact within a single examination. We therefore attempt to establish recommendations about preoperative imaging in patients with PEX.

Method: Chest computed tomography (CT), stress echocardiography (Echo), and cardiac magnetic resonance (CMR) allow the evaluation of specific information regarding structural and functional characteristics of vital importance to assess surgical candidacy and define surgical strategies. We sought to provide a multidisciplinary state of the art document involving thoracic surgeons, radiologists, and cardiologists; to establish recommendations about the variables to be included in the reports of the imaging examinations performed in patients with PEX.

Results: We provide recommendations for preoperative image acquisition and analysis, aimed at the assessment of the severity of the chest wall deformity (CT); the site of maximum cardiac compression, extent of increased interventricular dependence, and presence of pericardial effusion (CMR); and the effect of PEX on the functional capacity and exercise-related systolic and/or diastolic function, and tricuspid annulus compression (Echo).

Conclusions: This multidisciplinary state of the art document involving thoracic surgeons, radiologists, and cardiologists provides recommendations about preoperative imaging for patients with PEX.

1. Introduction

Pectus excavatum (PEX) is the most common chest wall malformation, and affects predominantly men [1,2]. This malformation, characterized by a depression of the sternum and adjacent cartilages, has been considered until recently only a cosmetic anomaly of the chest wall. However, PEX can also affect the quality of life of these patients, especially since the population most commonly involved are children, adolescents, and young adults [3–6]. Currently, the most widely established surgical correction strategy involves insertion of a retrosternal bar guided by thoracoscopy (Nuss procedure). This procedure, reserved for very specific situations, has shown to improve the quality of life of patients with PEX. [7,8].

In the last decade, several studies demonstrated that, in addition to the psychosocial impact, the depression of the anterior chest wall can also compress the right cardiac chambers, causing various morphological and functional cardiac alterations [9–11]. Although symptoms among these patients can be variable and sometimes subjective, a large proportion of patients with significant sternal depression may have symptoms related to physical exertion [3][10]. The underlying mechanisms responsible for the cardiopulmonary function impairment that can be found in PEX, although not fully elucidated, have been related to different morphological and functional findings, including: 1) dysfunction of respiratory biomechanics, with abdominal breathing and

* Corresponding autor at: Diagnóstico Maipú, Av. Maipú 1668, Vicente López (B1602ABQ), Buenos Aires, Argentina.
E-mail address: grodriguezgranillo@gmail.com (G.A. Rodríguez-Granillo).

https://doi.org/10.1016/j.ejrad.2019.06.014
Received 12 March 2019; Received in revised form 10 June 2019; Accepted 13 June 2019

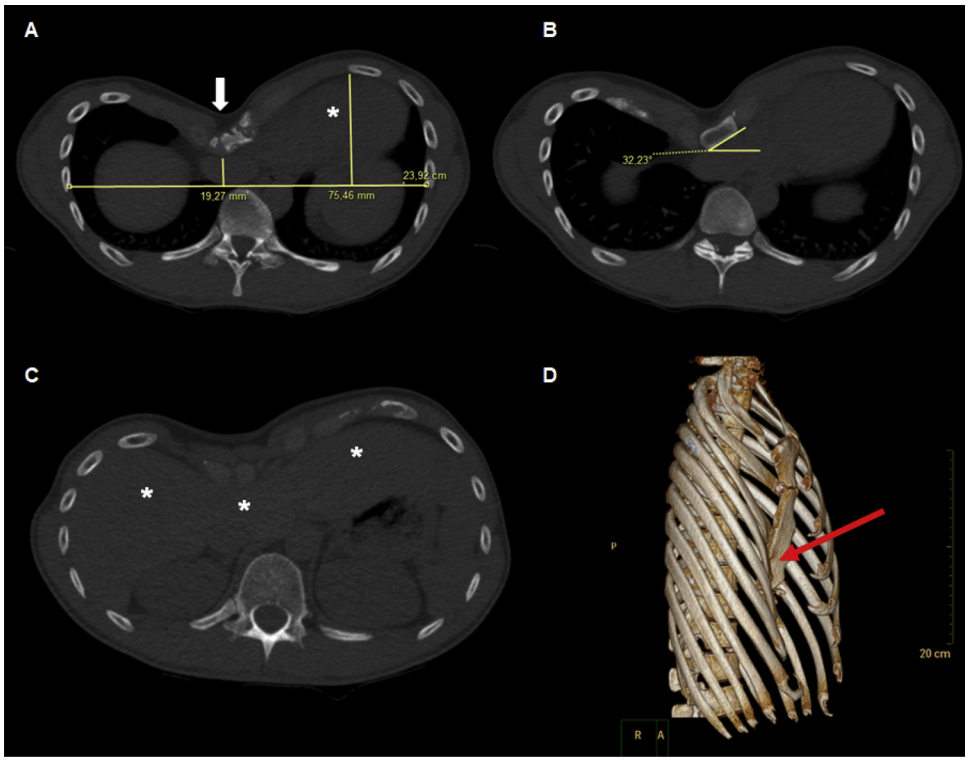

Fig. 1. Thirty-two year-old male patient with shortness of breath during exercise and pectus excavatum. Chest computed tomography revealed a Haller index of 12.4 and a correction index of 74% (panel A). Note the displacement of the cardiac silhouette towards the left hemithorax (asterisk in panel A), and a 32° right-sided sternal torsion (panel B). In the lower sections, compression of the liver by the depressed chest wall is evident (*, panel C). Three-dimensional reconstructions in these patients (panel D) are very useful for planning the surgical strategy, clearly demonstrating both depression and right-sided sternal torsion (arrow).

inability to achieve deep inspiration; 2) impairment of diastolic and/or systolic ventricular function; 3) a restrictive pulmonary function pattern [10,12].

Malformation of the chest wall in patients with PEX has various clinical phenotypes, including differences in the depth of the depression, thorax asymmetry, location of the site of maximum compression/depression, and different behavior throughout the respiratory cycle [13,14]. Therefore, no imaging modality can enable a comprehensive assessment of PEX severity and cardiac impact within a single examination. Chest computed tomography (CT), stress echocardiography, and cardiac magnetic resonance (CMR), usually necessary to plan and guide the surgical strategy, allow the evaluation of specific information regarding structural and functional characteristics [14,15]. However, image acquisition protocols and reports in this population differs significantly from routine examinations. Therefore, we sought to provide a multidisciplinary state of the art document involving thoracic surgeons, radiologists, and cardiologists to establish recommendations about preoperative imaging in this particular patient population.

2. Chest CT

In patients with PEX, CT allows determination of several thoracic indexes to assess the severity of the chest wall deformity and for determining candidacy for PEX repair, surgical strategies, and the selection of the type and size of the implants [13]. Three-dimensional reconstructions are essential for these decisions (Figs. 1 and 2). In this subset of patients, CT should be requested as three-dimensional, non-contrast, end-expiration chest CT.

2.1. Acquisition protocol

Chest CT scans should be performed at end expiration in order to calculate the most severe thoracic indexes in conditions similar to those observed by the surgeon in the operating room (patient relaxed at expiration) [16]. Given the youth of the population involved, efforts to limit the levels of exposure to ionizing radiation should be maximized. Therefore, CT acquisition protocols with a low voltage (80–100 kV), automatic tube current modulation, and iterative reconstruction algorithms should be advocated [17].

Although different anatomic indexes allow an objective estimation of the degree of chest wall deformity, no single index allows a comprehensive assessment of the type and severity of thoracic malformation in patients with PEX. [18]. In addition, the cut-off points for each of these anatomical indexes have not been fully elucidated. Anatomic indexes that should be calculated and included within chest CT reports of patients with PEX are summarized in Table 1.

2.2. Chest wall malformation indexes

2.2.1. Haller index

The Haller index (HI), usually calculated by CT, is the most commonly used anatomic index to establish PEX severity, and undoubtedly the most well-known and divulged assessment parameter among physicians who treat this deformity as well as outside the realm of thoracic wall surgeons [13,19].

For its calculation, two measurements of the chest wall should be obtained at the point of maximum sternal / costal cartilage depression: the minimum antero-posterior distance (APmin, shortest distance between the posterior aspect of the sternum/ costal cartilage and the anterior aspect of the vertebrae) and the maximum transverse distance (TD, the widest inner transverse diameter of the thoracic cage). Thus, the HI is calculated using the following formula: TD/APmin (Fig. 1). It should stressed that the site of maximum depression of the anterior chest wall does not always involve the sternum, but may be related to the interchondral joints.

Although the HI is highly reproducible and is commonly used to establish surgical candidacy (generally a HI $>$ 3.25), it has limitations that must be considered. First, the cutoff point of 3.25 is controversial due to phenotypic differences related to sex, age, and morphology of the rib cage. Indeed, in a series of 271 patients with surgical correction of PEX, no significant relationship was found between the HI and the operating time, length of hospitalization or infectious complications. [20]. Furthermore, beyond displaying a limited prognostic value, in some patients the HI cannot discriminate between patients with and

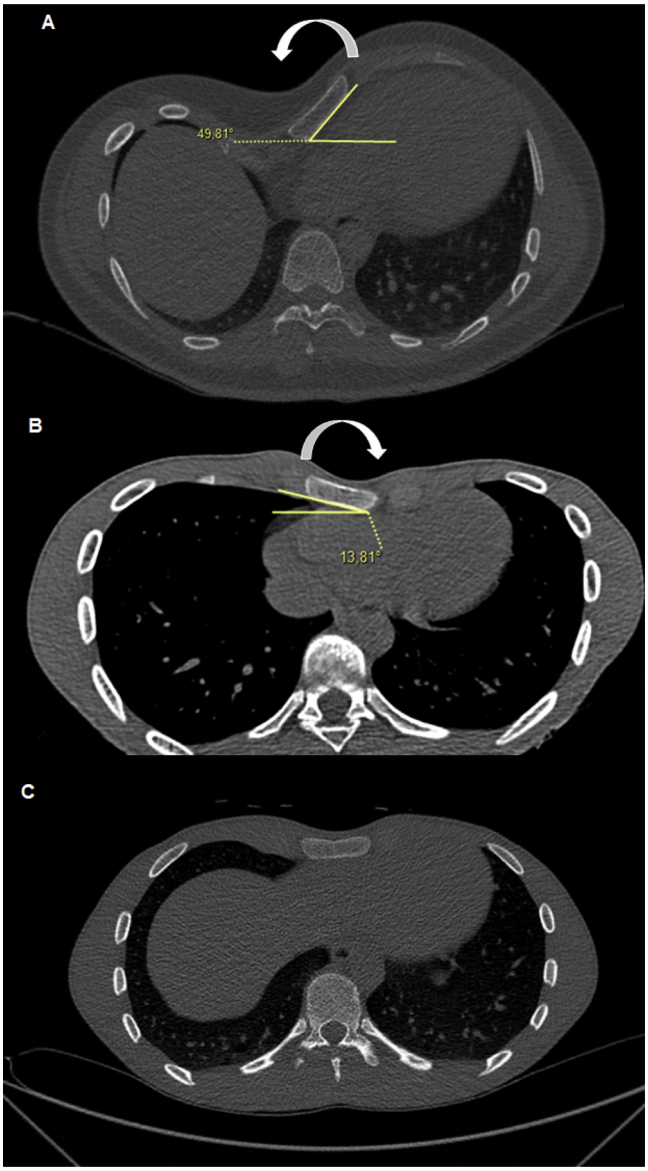

Fig. 2. Types of sternal torsion evaluated by chest computed tomography in three patients with pectus excavatum. Right sternal torsion of 49.8 degrees (panel A), left-sided torsion of 13.8 degrees (panel B), and patient without evidence of sternal torsion (panel C).

without PEX [13,19]. The HI does not consider the chest wall asymmetry, of vital importance in these patients; and does not quantify the depth of the depression. These limitations motivated the development of other anatomic indexes, such as the correction index (CI).

2.2.2. Correction index

The second thoracic index that should be included in CT reports is the correction index (CI) [13]. This index corresponds to the depth of the anterior wall depression, reflected as a percentage of the sternal/costal cartilage depression that should be corrected with surgery. For its calculation, a horizontal line should be extrapolated through the anterior border of the spine, and two measurements should be obtained: the APmin, and the largest inner anterior-posterior distance between such horizontal line and the most anterior portion of the chest wall (APmax). Thus, the CI is calculated using the following formula: [(APmax-APmin) / APmax] x 100 (Fig. 1).

It is noteworthy that the CI provides an estimation of the depth of the anterior wall defect independent of the width of the inner ribcage [13]. Moreover, the CI enables a more accurate discrimination between patients with and without PEX [21]. A CI > 10% identifies patients with PEX, and an CI > 20% identifies those with indication for surgical correction.

2.3. Other considerations

Aside from including the aforementioned anatomic indexes, CT reports should also indicate the presence or absence of sternal torsion, its orientation (right or left torsion), and severity (in degrees). Right sternal torsion is the most common form (Fig. 2). In addition, other considerations should be evaluated and reported including whether the defect is asymmetric, the presence of associated costal malformations, of pleural and/or pericardial effusion, and of the displacement of the cardiac silhouette or compression of the liver (Fig. 1, panel C). Table 1 summarizes the main findings that should be included in the CT reports in patients with PEX.

It is worth noting that thoracic surgeons appreciate three-dimensional reconstructions of the chest wall for planning the surgical strategy and to calculate the size and curvature of the retrosternal bar to be used. Accordingly, such reconstructions should be included within the CT reports.

3. Stress echocardiography

A non-negligible percentage of patients with PEX can have impaired functional capacity and exercise intolerance [6,8,22,23]. Despite several possible underlying mechanisms and a great variability between patients according to the malformation phenotype, exercise intolerance is generally attributed to external cardiac compression (specifically of the right ventricle) [24]. Baseline and stress echocardiography (stress-echo) allow the demonstration of such compression and its dynamics during rest and stress (exercise), manifested by a reduction in the diameter of the tricuspid annulus (and of the tricuspid/mitral annulus width ratio), a fixed tricuspid valve area in rest and stress, and by an increased tricuspid diastolic gradient (Fig. 3). Also, it is important to explore the presence of signs of diastolic dysfunction not only of the right ventricle, but also of the left (Fig. 3). Finally, the presence of paradoxical septal motion should also be evaluated (Fig. 4) [14].

In general, within the routine of echocardiography laboratories, the vast majority of patients undergo stress-echo to rule out ischemic heart disease or, to a much lesser extent, for other indications such as valvular heart disease. Therefore, stress-echo operators usually focus on ruling out stress-induced regional wall motion abnormalities and are not familiar with the specific characteristics of this population. Ideally, stress tests should be performed on a bicycle in supine position.

3.1. Standardization of stress-echo acquisition, analysis, and reports

Stress-echo, by definition, includes an exercise stress test. Therefore, it is of great value to document the maximum exercise capacity, quantified by the metabolic equivalents (METS) achieved. In a recent study, a lower maximum exercise capacity has been demonstrated in patients with PEX compared with controls (8.4 ± 2.0 METS vs. 15.1 ± 4.6 METS, $p < 0.0001$) [14]. The stress test is also a good opportunity to assess and record symptoms, particularly taking into account that these patients may be interrogated by pediatric surgeons unfamiliar with cardiac anamnesis. During baseline echocardiogram, aside from measuring the usual parameters, the presence of paradoxical septal motion (Fig. 3) should also be assessed. Furthermore, evaluation using the apical four-chamber view is encouraged, although occasionally the acoustic window can be troublesome due to thoracic

Table 1
Proposed summary findings to be included in study reports among patients with pectus excavatum.

	Imaging tests		
Findings to describe in the report	Chest computed tomography with 3D reconstruction	Stress echocardiography	Cardiac magnetic resonance (non-contrast)
Descriptive	Clinical history	Clinical history	Clinical history
	Type, symmetry, and severity of the defect	Stress test findings	Standard evaluation of cardiac morphology and systolic function
	Presence of associated sternal, costal, and chondral malformations	Echocardiographic findings (rest and stress)	Assessment of changes in septal motion throughout the respiratory cycle
	Presence of liver compression	Systolic and diastolic function	Assessment of compression of the RV elicited by chest wall depression
		Evaluation of septal motion	Rule out pericardial and/or pleural effusion
		Calculation of tricuspid valve area	Rule out valvular heart disease
Structured	Haller index	LV systolic function (rest/stress)*	Cardiac compression classification (types 0; 1; 2)
	Correction index	RV systolic function (rest/stress)*	Abnormal septal motion*
	Sternal torsion (degrees and orientation)	Signs of LV diastolic dysfunction (rest/stress)*	Incremented interventricular dependence (absence; increased left ventricular eccentricity; or septal flattening)
	Cardiac silhouette displacement*	Signs of RV diastolic dysfunction (rest/stress)*	Pericardial effusion*
	Cardiac silhouette deformation *	Increased tricuspid diastolic gradient during stress*	Pleural effusion*
		Paradoxical septal motion*	LV systolic dysfunction*
		Fixed tricuspid area*	RV systolic dysfunction*
Optional		Pulmonary artery systolic pressure (mmHg)	Tricuspid/mitral annulus width ratio
		Tricuspid/mitral annulus width ratio	

Note. *Normal/abnormal (or No/yes). RV: right ventricle. LV: left ventricle.

malformation. Baseline and stress measurements to be included in the report comprise: mean and peak tricuspid diastolic gradient (using continuous-wave Doppler); E wave and A wave of the tricuspid and mitral valves using pulsed-wave Doppler; and tricuspid e and a waves through tissue Doppler at the level of the tricuspid annulus and the interventricular septum (Fig. 3). In addition, the presence of any echocardiographic evidence of abnormal diastolic function at rest and/or stress should be reported, defined as one or more of the following parameters. Within the left ventricle: E/e ratio > 15; septal wave < 7 cm/s; tricuspid regurgitation velocity > 2.8 m/s. Within the right ventricle: e/a ratio < 0.6, and E/A ratio < 0.8. The presence of reversal of the mitral and/or tricuspid E/A and/or e/a ratios during exercise should be highlighted as signs of (some degree of) diastolic dysfunction of the left ventricle or right ventricle. Finally, the tricuspid area should be recorded at rest and stress (calculated by means of the continuity equation and using the right or left ventricular outflow tract as reference), the left ventricular (ejection fraction) and right ventricular (tricuspid annular plane systolic excursion) systolic function, and the S wave velocity using tissue Doppler of the tricuspid annulus.

Table 1 summarizes the main findings that should be included in stress-echocardiogram reports of patients with PEX.

4. Cardiac magnetic resonance

In patients with PEX, this examination should be requested as non-contrast CMR. Among patients with PEX, CMR comprises a brief protocol about 20 min duration, which includes scout views, cine imaging using steady state free precession (SSFP) sequences in four-chamber (horizontal long axis), two-chamber (vertical long axis), three-chamber (left ventricular outflow tract), and short-axis (from the mitral valve to the apex) views. These images must be acquired at end expiration. In addition, free-breathing "real time" cine images should be obtained at a single mid-short-axis view and a four-chamber view using balanced SSFP sequences with parallel acquisition techniques.

Using the aforementioned sequences, in addition to performing a standard CMR assessment including cardiac chamber dimensions, wall thickness, ventricular volumes and systolic function, the following specific parameters will be evaluated. On one hand, the presence and type of cardiac compression will be established according to a classification based on the definition of the site of greatest compression of the chest wall (sternal/sternal cartilage) on the right side of the heart using four-chamber views (3 slices) at end-diastole [25]. In this way, patients can be classified as: type 0, without cardiac compression; type 1, patients with compression of the right ventricle without involvement of the atrioventricular groove; and type 2, patients with compression of both the right ventricle and atrioventricular groove (Fig. 5). In addition, the presence of abnormal septal motion (particularly at early diastole) should be evaluated using all available planes, being the three and four-chamber views particularly useful for this purpose. Interventricular dependence should be assessed by means of free-breathing "real-time" short-axis cine images, using the slice with the greatest septal displacement for its evaluation. In patients with PEX, cardiac changes are exacerbated during inspiration, with inspiratory displacement of the interventricular septum towards the left or even septal flattening (Fig. 6) [14,26,27]. The underlying mechanism of such anomalous septal motion is the presence of a non-distensible right ventricle, which is restricted due to the sunk sternum and adjacent cartilages [26]. Real-time cine images enable the evaluation of septal motion across the respiratory cycle. Therefore, septal motion should be classified as follows, according to the presence and extent of increased interventricular dependence: 1) normal (normal septal motion, without significant changes during inspiration); 2) abnormal (paradoxical septal motion, without significant changes during inspiration); 3) increased left ventricular eccentricity (abnormal septal motion, and increased left ventricular eccentricity during inspiration); 4) septal flattening during inspiration (D-shaped left ventricle).

Ventricular eccentricity, originally described as a surrogate for right ventricular overload and septal excursion to the left, is calculated as the ratio between the upper-lower and anterior-posterior distances of the left ventricle at end-diastole (Fig. 6) [28].

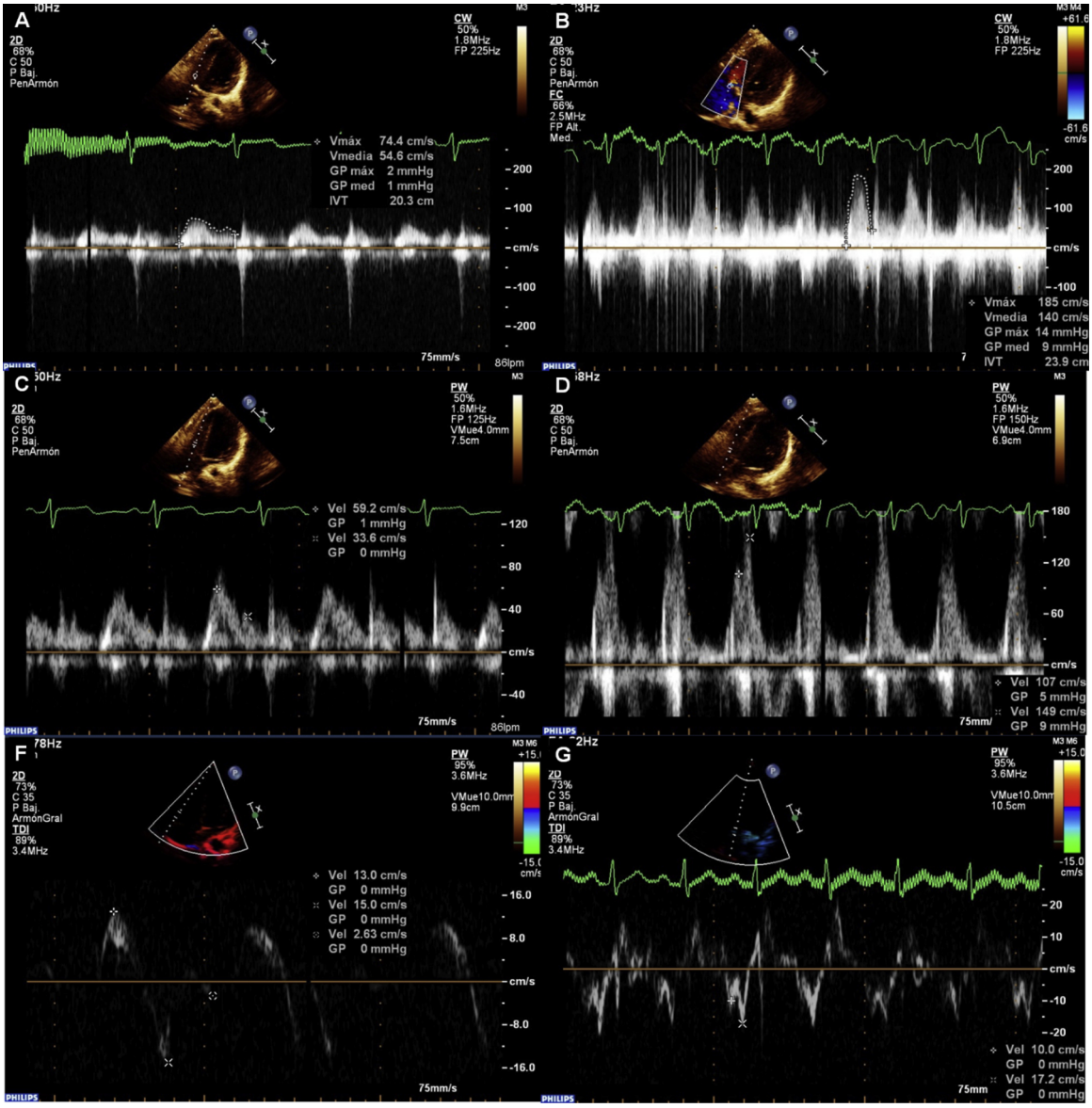

Fig. 3. Increase of tricuspid diastolic gradient and diastolic dysfunction in a patient with pectus excavatum, evaluated by Doppler echocardiography. Tricuspid diastolic gradient at rest (panel A) and stress (panel B). The pattern of tricuspid filling is normal at rest (panels C and F), with diastolic dysfunction at stress demonstrated by inversion of E/A (panel D) and e/a (panel G) ratios.

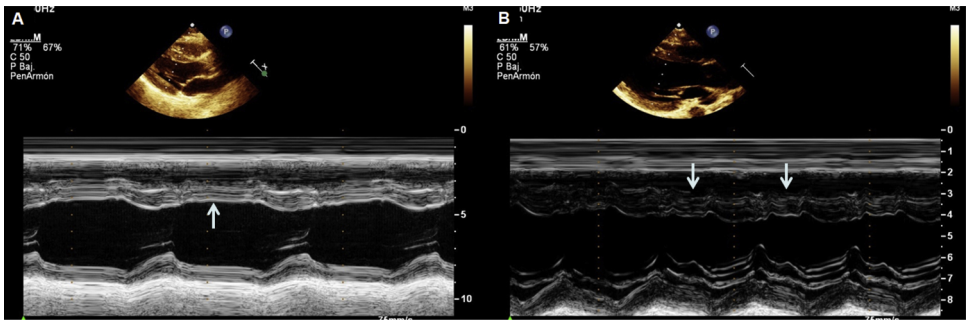

Fig. 4. Evaluation of septal wall motion in patients with pectus excavatum using M-mode echocardiography. Normal motion, without diastolic impairment of septal motion (panel A, arrow). Paradoxical septal motion, with abnormal motion during diastole (arrows in panel B).

4.1. Ancillary evaluations

A significant proportion of patients with PEX may have pericardial effusion, which is generally mild (Fig. 6). The presence of pericardial effusion should be evaluated in diastole, and it should be noted that a minimum amount of physiological fluid at a basal inferior (oblique sinus) or apical locations should not be considered as effusion [29]. In a smaller proportion of patients, minimal pleural effusion can be detected.

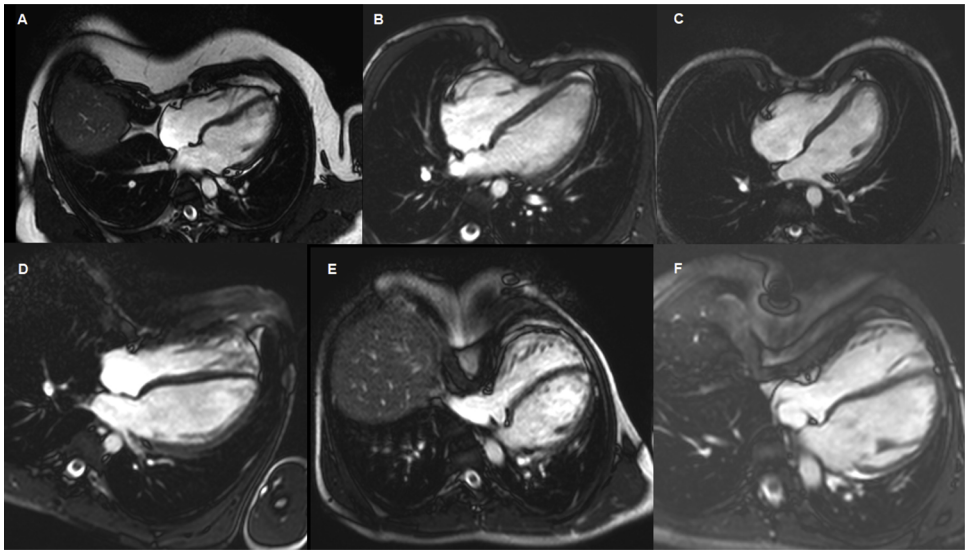

Fig. 5. Types of cardiac compression in six different patients with pectus excavatum evaluated by cardiac magnetic resonance. Patient without cardiac compression (type 0, panel A); two patients with compression of the right ventricle (type 1, panels B and C), and three patients with compression of both the right ventricle and atrioventricular groove (type 2, panels D–F). Note that in type 2 compression depicted in panel D, a diffuse compression involving the right atrium, atrioventricular groove, and right ventricle is present.

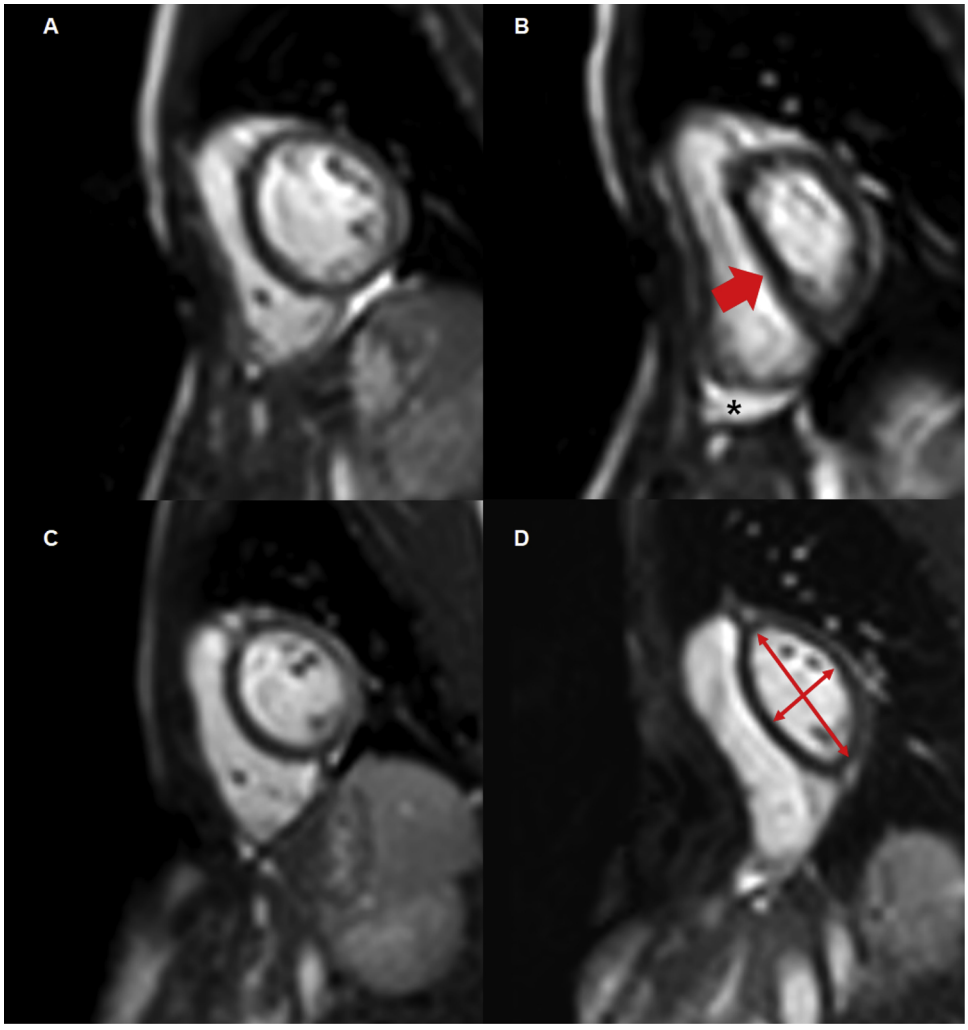

Fig. 6. Patients with increased interventricular dependence identified by cardiac magnetic resonance using free-breathing "real-time" cine imaging. During expiration (panels A and C), the left ventricle has a normal symmetric morphology with similar transverse and superior-inferior diameters. In the first case (panels A and B), there is a marked excursion of the interventricular septum to the left during inspiration, with septal flattening (panel B). This patient also has mild pericardial effusion (asterisk). In the second case (panels C and D), a marked increase in left ventricular eccentricity was observed during inspiration (panel D), with no evidence of septal flattening.

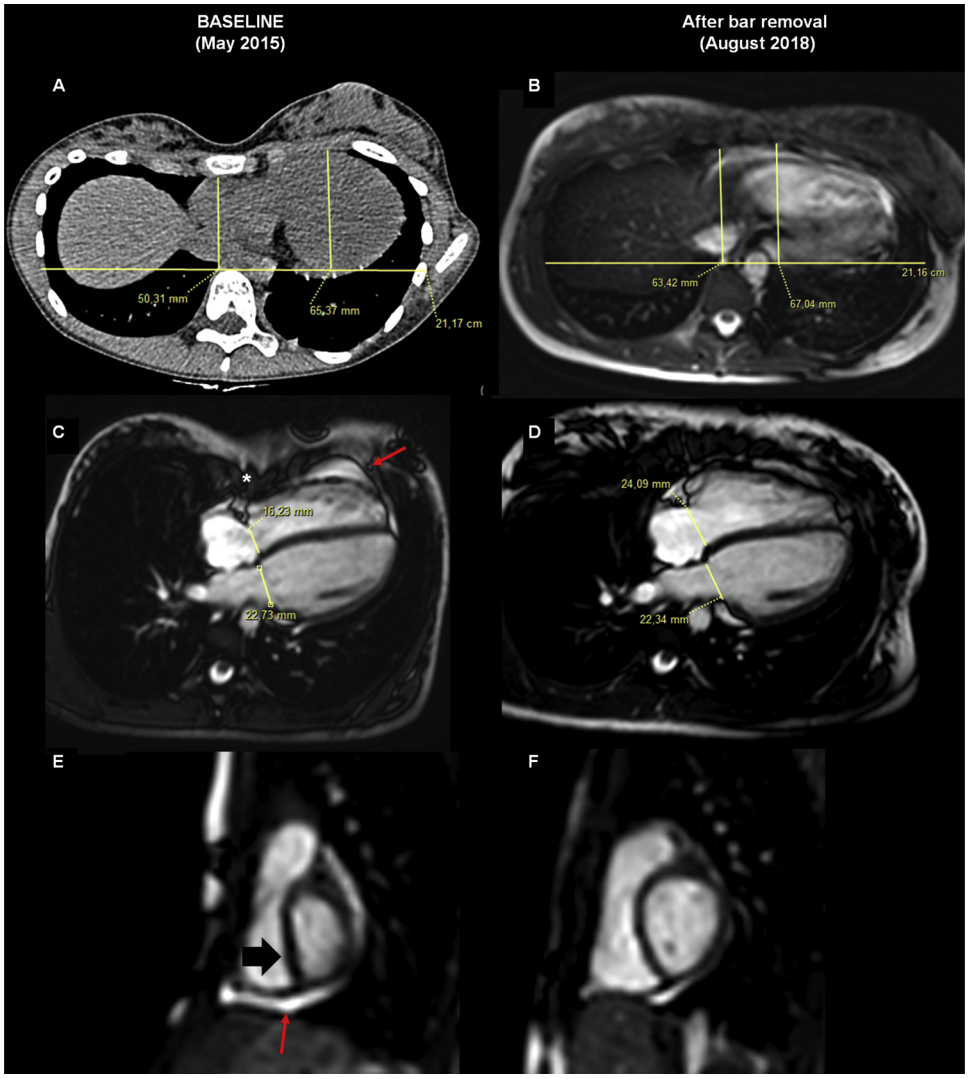

Fig. 7. Fourteen-year-old female with pectus excavatum and indication for surgical correction using a Nuss minimally invasive technique (retrosternal bar implant guided by thoracoscopy) in May 2015. Chest computed tomography was performed as part of preoperative surgical evaluation (panel A) as well as a cardiac magnetic resonance (CMR, panels C and E). After removing the retrosternal bar 3 years later, a control CMR was performed (panels B, D, and F). Note the improvement in the Haller index (baseline: 4.2, follow-up: 3.3) and in the correction index (baseline: 23%, follow-up: 5%). Absence of cardiac compression at follow-up is also observed (panel D), evidencing a type 2 compression at baseline (asterisk in panel C). At baseline, these same four-chamber planes showed pericardial effusion (red arrows in panels C and E) and compression of the tricuspid annulus manifested by a tricuspid/mitral annulus width ratio of 0.71 at baseline and of 1.08 at follow-up. Finally, the presence of septal flattening at baseline (panel E, black arrow) is highlighted, which was resolved at follow-up (panel F).

Albeit optional, the assessment of the tricuspid and mitral annulus width can be valuable to evaluate structural changes in case of an eventual surgical correction. These measurements should be performed using the four-chamber view at the end of diastole, with a normal value of the tricuspid/mitral annulus width ratio of more than 0.90. This measure could be particularly useful for follow-up imaging of operated patients (Fig. 7).

Finally, images of axial locators (scout) could be used to calculate the anatomical indexes described previously (HI and CI), this being of particular relevance in patients without previous CT or those in whom it is desired to avoid ionizing radiation (Fig. 7) [30].

Table 1 summarizes the main findings that should be included in CMR reports among patients with PEX.

5. Final considerations and future perspectives

In general, though yet to be established, the surgical decision in patients with PEX is based upon the presence of at least two of the following criteria: 1) HI larger than 3.25, and/or a CI larger than 20%; 2) exercise-related symptoms; 3) pulmonary manifestations (atelectasis, bronchiectasis, repetitive pneumonia); 4) significant cardiac compression [evidence of cardiac compression (type 1 or 2) and one or more of the following: systolic dysfunction, inspiratory septal flattening, moderate pericardial effusion, signs of diastolic dysfunction at stress, or elevated trans-tricuspid gradient at stress (mean gradient $\geq$6 mmHg)].

In recent years, the demonstration of the impact of chest wall depression not only on the aesthetic and psychosocial aspects of patients, but also on their cardiopulmonary function, has increased the concurrence of patients with PEX for imaging examinations. Most of these patients are referred by thoracic surgeons who seek a preoperative evaluation of the morphological and/or functional impact of the malformation on the heart. Despite this, there is limited knowledge about the importance of making specific image acquisitions and measurements among these patients.

Accordingly, the standardization of the reports that we propose within this document seeks to provide, from the standpoint of the professionals involved in the diagnosis and treatment of the PEX, some guidance to acquire and report the imaging methods concerned, with the final objective of improving the diagnosis and treatment of these patients.

In terms of future perspectives, it is expected that the use of three-dimensional optical scanning with virtual reconstruction will increase in the near future for the diagnosis, characterization and follow up of patients with thoracic wall deformities (Fig. 8). Early studies using this radiation-free technology have shown promising findings [31–33]. In the same line, three-dimensional printing may play an important role in the future of chest wall surgery, not only for surgical simulation including estimation of the number and location of bars needed, but also for the development of prosthetic models [34].

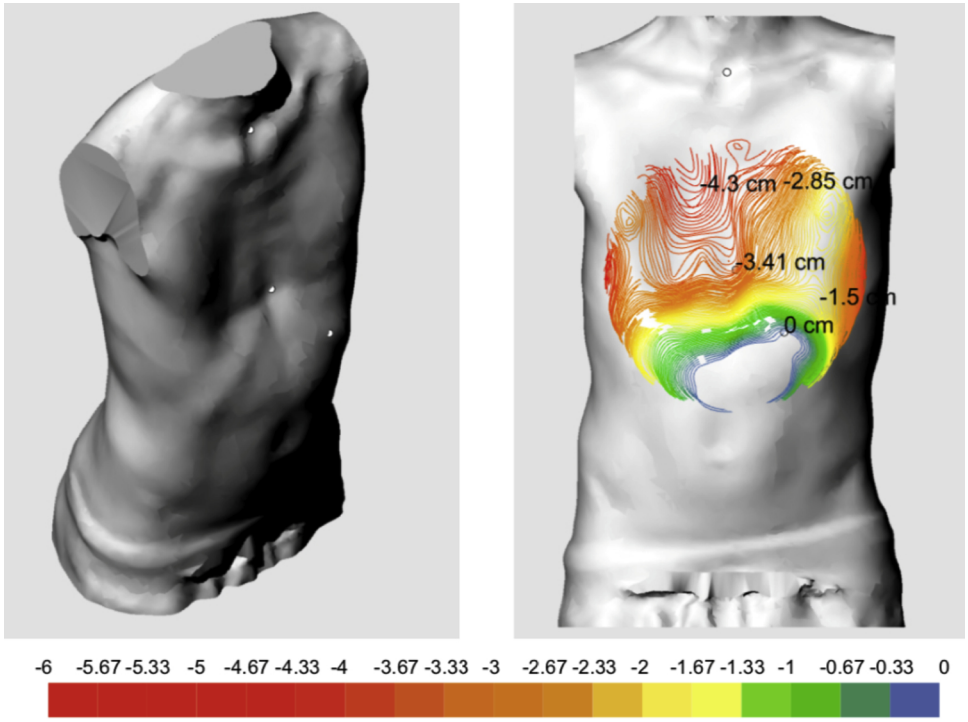

Fig. 8. Three-dimensional optical scanning of a patient with pectus excavatum. The regional depth and asymmetry of the malformation can be clearly depicted. Structured white light scanners (WLS) operate by projecting a grid onto an object, then analyze the pattern distortion on the object's surface to identify a series of points by which to orient itself. Triangulation is then used to determine the distances between points on that grid to reconstruct the object as a digital mesh. Image quality can be achieved with precision to a resolution of 0.5 mm. Without using ionizing radiation, WLS may be safely used in preoperative severity assessment and particularly for repeated scanning among patients requiring long term monitoring.

Declaration of competing interest

None of the authors have conflicts of interest to declare

References

[1] J.M. Cobben, R.J. Oostra, F.S. van Dijk, Pectus excavatum and carinatum, Eur. J. Med. Genet. 57 (8) (2014) 414–417.

[2] C. Brochhausen, S. Turial, F.K. Muller, V.H. Schmitt, W. Coerdt, J.M. Wihlm, et al., Pectus excavatum: history, hypotheses and treatment options, Interact. Cardiovasc. Thorac. Surg. 14 (6) (2012) 801–806.

[3] Y. Ji, W. Liu, S. Chen, B. Xu, Y. Tang, X. Wang, et al., Assessment of psychosocial functioning and its risk factors in children with pectus excavatum, Health Qual. Life Outcomes 9 (2011) 28.

[4] J.J. Lomholt, E.B. Jacobsen, M. Thastum, H. Pilegaard, A prospective study on quality of life in youths after pectus excavatum correction, Annals Cardiothorac Surg 5 (5) (2016) 456–465.

[5] K. Bostanci, M.H. Ozalper, B. Eldem, M.O. Ozyurtkan, A. Issaka, N.O. Ermerak, et al., Quality of life of patients who have undergone the minimally invasive repair of pectus carinatum, Eur. J. Cardiothorac. Surg. 43 (1) (2013) 122–126.

[6] R.E. Kelly Jr., T.F. Cash, R.C. Shamberger, K.K. Mitchell, R.B. Mellins, M.L. Lawson, et al., Surgical repair of pectus excavatum markedly improves body image and perceived ability for physical activity: multicenter study, Pediatrics 122 (6) (2008) 1218–1222.

[7] D. Nuss, R.J. Obermeyer, R.E. Kelly, Nuss bar procedure: past, present and future, Annals Cardiothorac Surg 5 (5) (2016) 422–433.

[8] R.E. Kelly Jr., R.B. Mellins, R.C. Shamberger, K.K. Mitchell, M.L. Lawson, K.T. Oldham, et al., Multicenter study of pectus excavatum, final report: complications, static/exercise pulmonary function, and anatomic outcomes, J. Am. Coll. Surg. 217 (6) (2013) 1080–1089.

[9] R.E. Kelly Jr., A. Daniel, Outcomes, quality of life, and long-term results after pectus repair from around the globe, Sem. Pediatr. Surg. 27 (3) (2018) 170–174.

[10] D.E. Jaroszewski, C.S. Velazco, V. Pulivarthi, R. Arsanjani, R.J. Obermeyer, Cardiopulmonary Function in Thoracic Wall Deformities: What Do We Really Know? Eur. J. Pediatr. Surg. 28 (4) (2018) 327–346.

[11] M. Maagaard, M. Tang, S. Ringgaard, H.H. Nielsen, J. Frokiaer, M. Haubuf, et al., Normalized cardiopulmonary exercise function in patients with pectus excavatum three years after operation, Ann. Thorac. Cardiovasc. Surg. 96 (1) (2013) 272–278.

[12] T. Abu-Tair, S. Turial, M. Hess, C.M. Wiethoff, G. Staatz, A. Lollert, et al., Impact of pectus excavatum on cardiopulmonary function, Ann. Thorac. Cardiovasc. Surg. 105 (2) (2018) 455–460.

[13] J.A. Sujka, S.D. St Peter, Quantification of pectus excavatum: anatomic indices, Sem. Pediatr. Surg. 27 (3) (2018) 122–126.

[14] G.A. Rodriguez-Granillo, I.M. Raggio, A. Deviggiano, G. Bellia-Munzon, C. Capunay, M. Nazar, et al., Impact of pectus excavatum on cardiac morphology and function according to the site of maximum compression: effect of physical exertion and respiratory cycle, Eur. Heart J. Cardiovasc. Imaging (April) (2019), https://doi.org/10.1093/ehjci/jez061 pii: 5425270.

[15] S. Oezcan, C.H. Attenhofer Jost, M. Pfyffer, C. Kellenberger, R. Jenni, C. Binggeli, et al., Pectus excavatum: echocardiography and cardiac MRI reveal frequent pericardial effusion and right-sided heart anomalies, Eur. Heart J. Cardiovasc. Imaging 13 (8) (2012) 673–679.

[16] M. Albertal, J. Vallejos, G. Bellia, C. Millan, F. Rabinovich, E. Buela, et al., Changes in chest compression indexes with breathing underestimate surgical candidacy in patients with pectus excavatum: a computed tomography pilot study, J. Pediatr. Surg. 48 (10) (2013) 2011–2016.

[17] Z.U. Sarwar, R. DeFlorio, S.C. O'Connor, Pectus excavatum: current imaging techniques and opportunities for dose reduction, Sem Ultrasound CT MR 35 (4) (2014) 374–381.

[18] M. Martinez-Ferro, Indexes for pectus deformities, in: S. Kolvekar, H. Pilegaard (Eds.), Chest Wall Deformities and Corrective Procedures, Springer, Cham, 2016.

[19] J.A. Haller Jr., S.S. Kramer, S.A. Lietman, Use of CT scans in selection of patients for pectus excavatum surgery: a preliminary report, J. Pediatr. Surg. 22 (10) (1987) 904–906.

[20] V.E. Mortellaro, C.W. Iqbal, F.B. Fike, S.W. Sharp, D.J. Ostlie, C.L. Snyder, et al., The predictive value of Haller index in patients undergoing pectus bar repair for pectus excavatum, J. Surg. Res. 170 (1) (2011) 104–106.

[21] S.D. St Peter, D. Juang, C.L. Garey, C.A. Laituri, D.J. Ostlie, R.J. Sharp, et al., A novel measure for pectus excavatum: the correction index, J. Pediatr. Surg. 46 (12) (2011) 2270–2273.

[22] D. Jaroszewski, D. Notrica, L. McMahon, D.E. Steidley, C. Deschamps, Current management of pectus excavatum: a review and update of therapy and treatment recommendations, J. Am. Board Fam. Med. 23 (2) (2010) 230–239.

[23] E. Coln, J. Carrasco, D. Coln, Demonstrating relief of cardiac compression with the Nuss minimally invasive repair for pectus excavatum, J. Pediatr. Surg. 41 (4) (2006) 683–686.

[24] R.J. Obermeyer, N.S. Cohen, D.E. Jaroszewski, The physiologic impact of pectus excavatum repair, Sem. Pediatr. Surg. 27 (3) (2018) 127–132.

[25] A. Deviggiano, P. Carrascosa, J. Vallejos, G. Bellia-Munzon, N. Vina, G.A. Rodriguez-Granillo, et al., Relationship between cardiac MR compression classification and CT chest wall indexes in patients with pectus excavatum, J. Pediatr. Surg. 53 (11) (2018) 2294–2298.

[26] A. Deviggiano, J. Vallejos, N. Vina, M. Martinez-Ferro, G. Bellia-Munzon, P. Carrascosa, et al., Exaggerated interventricular dependence among patients with pectus excavatum: combined assessment with cardiac MRI and chest CT, AJR Am. J. Roentgenol. 208 (4) (2017) 854–861.

[27] M. Francone, S. Dymarkowski, M. Kalantzi, F.E. Rademakers, J. Bogaert, Assessment of ventricular coupling with real-time cine MRI and its value to differentiate constrictive pericarditis from restrictive cardiomyopathy, Eur. Radiol. 16 (4) (2006) 944–951.

[28] M.Y. Abd El Rahman, W. Hui, F. Dsebissowa, S. Schubert, M. Gutberlet, R. Hetzer, et al., Quantitative analysis of paradoxical interventricular septal motion following corrective surgery of tetralogy of fallot, Pediatr. Cardiol. 26 (4) (2005) 379–384.

[29] J. Bogaert, M. Francone, Pericardial disease: value of CT and MR imaging, Radiology 267 (2) (2013) 340–356.

[30] N.A. Vina, P. Carrascosa, V.C. Mogensen, A. Deviggiano, G. Bellia-Munzon, M. Martinez-Ferro, et al., Evaluation of pectus excavatum indexes during standard cardiac magnetic resonance: potential for single preoperative tool, Clin. Imaging 53

(2018) 138–142.
[31] D. Szafer, J.S. Taylor, A. Pei, V. de Ruijter, H. Hosseini, S. Chao, et al., A simplified method for three-dimensional optical imaging and measurement of patients with chest wall deformities, J. Laparoendosc. Adv. Surg. Tech. A. 29 (2) (2019) 267–271.
[32] E. Port, F. Hebal, C.J. Hunter, B. Malas, M. Reynolds, Measuring the impact of brace intervention on pediatric pectus carinatum using white light scanning, J. Pediatr. Surg. 53 (12) (2018) 2491–2494.
[33] R.E. Kelly Jr., R.J. Obermeyer, M.A. Kuhn, F.W. Frantz, M.F. Obeid, N. Kidane, et al., Use of an optical scanning device to monitor the progress of noninvasive treatments for chest wall deformity: a pilot study, Korean J. Thorac. Cardiovasc. Surg. 51 (6) (2018) 390–394.
[34] N. Matsuo, K. Matsumoto, Y. Taura, Y. Sakakibara, D. Taniguchi, K. Takagi, et al., Initial experience with a 3D printed model for preoperative simulation of the Nuss procedure for pectus excavatum, J. Thorac. Dis. 10 (2) (2018) E120–E124.